JOC Article

Polyfunctional Recognition of Pyridinedicarboxylate Anions with Macrocyclic Polyamine Receptors Containing Heteroaromatic Groups

Carla Bazzicalupi,[†] Andrea Bencini,[†] Antonio Bianchi,*[,†] Claudia Borri,[†] Andrea Danesi,[†] Enrique Garcia-España,*[,‡] Claudia Giorgi,[†] and Barbara Valtancoli[†]

Department of Chemistry, Polo Scientifico, University of Florence, Via della Lastruccia 3, 50019 Sesto Fiorentino, Italy, and Departamento de Quimica Inorgánica, Instituto de Ciencia Molecular, Universidad de Valencia, Valencia, Spain

antonio.bianchi@unifi.it; enrique.garcia-es@uv.es

Received June 30, 2008

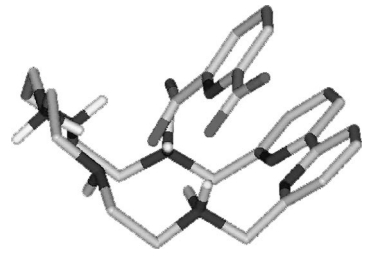

The interaction of the biologically relevant anions deriving from the six pyridinedicarboxylic acids (H_2PDC) with two macrocyclic receptors containing a pentamine chain and a bipyridine (**1**) or a phenanthroline (**2**) moiety, as well as with the aliphatic analogue [21]aneN_7 (**3**), was studied by means of spectroscopic methods (UV−vis, NMR) and potentiometric titrations affording the stability constants of the adducts formed. All three receptors form stable complexes with the substrates thanks to the formation of several salt bridges and hydrogen bond contacts, as observed in the crystal structure of the H_8[**3**(2,6-PDC)$_4$]·H_2O·0.5EtOH solid compound. Additional π-stacking interactions between the aromatic moieties of substrates and receptors enhance the stability of complexes with **1** and **2**. Compounds **1** and **2** show a marked selectivity toward 2,6- pyridinedicarboxylate anions. In particular, **1** is able to perform a very efficient recognition of these species in the presence of **2** and **3**. Molecular modeling calculations suggested that such recognition ability of **1** can be ascribed to a superior structural and electrostatic complementarity with the substrate compared to **2** and **3**.

Introduction

Design and synthesis of artificial receptors for the recognition of anionic substrates have contributed to the development of the new area of "anion coordination chemistry", whose interdisciplinary character spans from chemistry to biology and to new material sciences.[1−7]

Polyfunctional anions, namely anionic species containing binding sites of different natures, are challenging targets in recognition processes since they require complementary polyfunctional receptors which, in general, are not readily available but can be obtained only after careful design and lengthy syntheses from molecular fragments. Anions deriving from pyridinedicarboxylic acids (H_2PDC, Scheme 1) are an example of this kind of substrate.

Depending on the solution pH, they may exist as completely deprotonated dianionic species or as zwitterionic forms with one deprotonated carboxylic group and protonated pyridine

[†] University of Florence.
[‡] Universidad de Valencia.

(1) (a) Sessler, J. L.; Gale, P. A.; Cho, W. S. *Anion Receptor Chemistry (Monographs in Supramolecular Chemistry)*; Stoddart, J. F., Ed.; RSC: Cambridge, UK, 2006. (b) *Supramolecular Chemistry of Anions*; Bianchi, A., Bowman-James, K., Garcia-España, E., Ed.; Wiley-VCH: New York, 1997.
(2) Kubik, S.; Reyheller, C.; Stüwe, S. *J. Incl. Phenom. Macrocycl. Chem.* **2005**, *52*, 137–187.
(3) *Encyclopedia of Supramolecular Chemistry*; Atwood, J. L., Steed, J. W., Ed.; Marcel Dekker: New York, 2004.
(4) Special Issue on Anion Coordination Chemistry. *Coord. Chem. Rev.* **2003**, *240*, 1−226.
(5) Gale, P. A. *Coord. Chem. Rev.* **2001**, *213*, 79–128.
(6) Beer, P. D.; Gale, P. A. *Angew. Chem., Int. Ed.* **2001**, *40*, 487–516.
(7) Schmidtchen, F. P.; Berger, M. *Chem. Rev.* **1997**, *97*, 1609–1646.

10.1021/jo801366w CCC: $40.75
Published on Web 10/08/2008

SCHEME 1. Pyridinedicarboxylic Acids (H_2PDC)

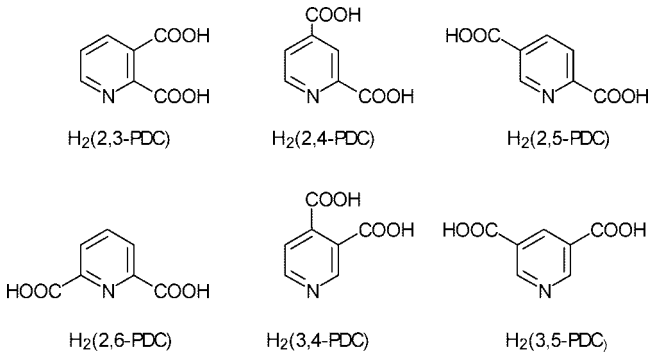

nitrogen or as species with two carboxylate and one ammonium groups. Furthermore, the positively charged species with two carboxylic groups and protonated pyridine nitrogen also may exist in very acidic solutions.

2,3-Pyridinedicarboxylic (H_2(2,3-PDC)) and 2,6-pyridinedicarboxylic (H_2(2,6-PDC)) acids are naturally occurring compounds. H_2(2,3-PDC) is a neurotoxic tryptophan metabolite, produced mainly by immune-activated macrophages, which is known to be involved in the pathogenesis of several major inflammatory neurological diseases (bacterial, viral, fungal, and parasitic infections, meningitis, septicaemia).[8] Furthermore, markedly increased concentrations of H_2(2,3-PDC) were found in cerebrospinal fluid of patients infected with clinically overt AIDS dementia complex.[9] H_2(2,6-PDC) is produced and secreted by several entomopathogenic fungi[10,11] and certain penicillium strains[12] and has been shown to act as an insecticidal toxin.[11,13] It is also the major chemical component of bacterial spores, including those of *Bacillus anthracis*, accounting for up to 15% of their weight, and it is involved in the peculiar stability, dormancy, germination, and resistance to heat and to ultraviolet and gamma radiations characteristic of this type of specialized cells.

Detection of these pyridinedicarboxylic acids is, of course, an important analytical issue, in particular after the potential use of *Bacillus anthracis* spores as a biological warfare agent was proposed. Since the presence of H_2(2,6-PDC) is considered diagnostic for the bacterial endospores, many analytical methods based on the detection of this molecule have been developed.[14] In particular, a potentiometric chemosensor based on selective detection of H_2(2,6-PDC) was recently prepared for the rapid identification of such a biological weapon.[15]

Taking into account the interest toward these substrates, we studied the possibility of performing recognition of the different pyridinedicarboxylic isomers by using the two polyfunctional

SCHEME 2. Macrocyclic Polyamine Receptors 1−3

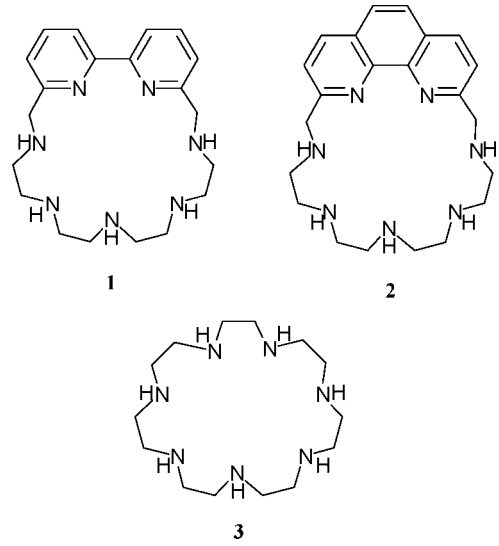

macrocyclic receptors **1** and **2** (Scheme 2), containing a common aliphatic pentaamine chain and two different heteroaromatic units. These receptors form highly protonated species in solution, in a large pH range, which can be used to bind the anionic forms of pyridinedicarboxylic acids through the formation of salt bridges and hydrogen bonds, while the heteroaromatic groups could be involved in stacking,[16] and cation−π[17] interactions with substrate pyridine or pyridinium groups and hydrophobic effects may favor their association. In order to analyze the role played by the heteroaromatic components of these receptors in the recognition process, we have also considered the purely aliphatic analogue **3** (Scheme 2). We report here the results of this study.

Results and Discussion

Crystal Structure of H_8[3(2,6-PDC)$_4$]·H_2O·0.5EtOH. The crystal structure consists of protonated receptor molecules, pyridinedicarboxylate anions, and water solvent molecules. The asymmetric unit contains two crystallographically nonequivalent protonated macrocyclic receptor molecules (indicated with **3a** and **3b**), each interacting via H-bonds with four anions, and two water molecules.

Figure 1 shows the ORTEP drawing of the receptors with the interacting anions, hereafter indicated as A−H, in agreement with the atom labeling. Selected H-bond distances for the interaction of **3a** and **3b** with A, B, C, D and E, F, G, H, respectively, are reported in the Supporting Information (Table S1).

(8) (a) Guillemin, G. J.; Meininger, V.; Brew, B. J. *Neurodegenerative Dis.* **2005**, *2*, 166–176. (b) El-Defrawy, S. R.; Boegman, R. J.; Jhamandas, K.; Beninger, R. J. *Can. J. Physiol. Pharmacol.* **1986**, *64*, 369–375. (c) Heyes, M. P.; et al. *Brain* **1992**, *115*, 1249–1273. (d) Stone, T. W.; Perkins, M. N. *Eur. J. Pharmacol.* **1981**, *72*, 411–412. (e) Schwarcz, R.; Whetsell, W. O., Jr.; Mangano, R. M. *Science* **1983**, *219*, 316–318. (f) Stone, T. W. *Pharmacol. Rev.* **1993**, *45*, 309–379.

(9) (a) Anderson, E.; Zink, W.; Xiong, H.; Gendelman, H. E. *J. Acquir. Immun. Def. Synd.* **2002**, *31* (Suppl. 2), S43–54. (b) Heyes, M. P.; Brew, B. J.; Martin, A.; Price, R. W.; Salazar, A. M.; Sidtis, J. J.; Yergey, J. A.; Mouradian, M. M.; Sadler, A. E.; Keilp, J.; Rubinow, D.; Markey, S. P. *Ann. Neurol.* **1991**, *29*, 202–209.

(10) Shima, M. *Bull. Sericult. Exp. Stat.* **1955**, *14*, 427–449.

(11) Claydon, N.; Grove, J. *J. Invertebr. Pathol.* **1982**, *40*, 413–418.

(12) (a) Oyama, J. *Rep. Ferment. Res. Inst.* **1961**, *20*, 95–103. (b) Oyama, J.; Nakamura, N.; Tanabe, O. *Rep. Ferment. Res. Inst.* **1961**, *19*, 5–81.

(13) Asaffz, A.; Cerda-Garcia-Rojas, C.; De la Torre, M. *Appl. Microbiol. Biotechnol.* **2005**, *68*, 542–547.

(14) (a) Vullev, V. I.; Jones, G. *Proceedings of the 222nd ACS National Meeting*, American Chemical Society: Washington, DC, 2000; INOR-557. (b) Scott, I. R.; Ellar, D. J. *J. Bacteriol.* **1978**, *135*, 133–137. (c) Goodacre, R.; Shann, B.; Gilbert, R. J.; Timmins, E. M.; McGovern, A. C.; Alsberg, B. K.; Kel, l D. B.; Logan, N. A. *Anal. Chem.* **2000**, *72*, 119–127. (d) Paulus, H. *Anal. Biochem.* **1981**, *114*, 407–410. (e) Fell, N. F.; Pellegrino, P. M.; Gillespie, J. B. *Anal. Chim. Acta* **2001**, *426*, 43–50. (f) Pellegrino, P. M.; Fell, N. F.; Rosen, D. L.; Gillespie, J. B. *Anal. Chem.* **1999**, *70*, 1755–1760. (g) Beverly, M. B.; Voorthees, K. J.; Hadfield, T. L.; Cody, R. B. *Anal. Chem.* **2000**, *72*, 2428–2432. (h) Hindle, A. A.; Hall, E. A. H. *Analyst* **1999**, *124*, 1599–1604. (i) Snyder, A. P.; Thornton, S. N; Dworzanski, J. P.; Meuzelaar, H. L. C. *Field Anal. Chem. Technol.* **1996**, *1*, 49–59.

(15) Zhou, Y.; Yu, B.; Levon, K. *Biosens. Bioelectron.* **2005**, *20*, 1851–1855.

(16) Hunter, C. A.; Lawson, K. R.; Perkins, J.; Urch, C. J. *J. Chem. Soc., Perkin Trans. 2* **2001**, 651–669.

(17) (a) Dougherty, D. A. *Science* **1996**, *271*, 163–168. (b) Ma, J. C.; Dougherty, D. A. *Chem. Rev.* **1997**, *97*, 1303–1324.

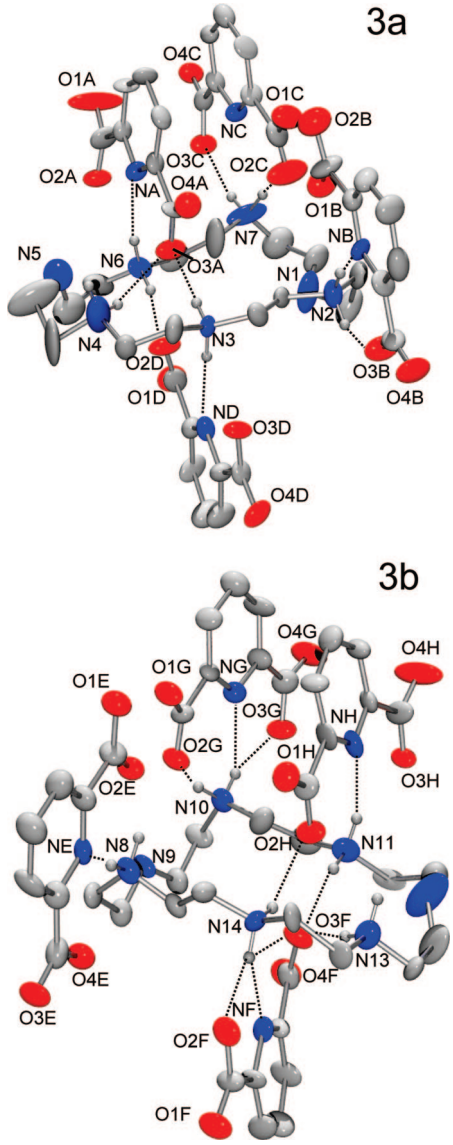

FIGURE 1. ORTEP drawing of **3a** and **3b** crystallographically nonequivalent macrocyclic receptors in the crystal structure of H_8[**3**(2,6-PDC)$_4$]·H_2O·0.5EtOH together with the interacting substrate anions.

Compounds **3a** and **3b** adopt rather flattened conformations (max deviation from the mean plane 0.94(1) Å for N1 (**3a**) and 0.726(7) Å N9 (**3b**)), mainly differing in the torsional angular values (see Supporting Information, Table S2). In particular, **3a** interacts with A, B, and C on one side and with D on the other side. All four substrate anions involve at least one carboxylic oxygen in the H-bond interaction with the protonated receptor. A, B, and D form also H-bond interactions with the receptor involving the pyridine nitrogens. A mutual disposition of protonated receptor molecules and anions similar to that found for **3a** is also observed for **3b** (Figure 1). In fact, E, G, and H are localized on the same side of the protonated receptor, while F lies on the opposite side. The H-bond network connecting receptor and substrate molecules is similar to that observed for **3**a, with F, G and H involving both pyridine nitrogens and carboxylic oxygens in hydrogen bonding.

The ΔF map carried out in the last refinement step did not allow us to localize the acidic protons. However, inspection of the crystal packing (see Supporting Information, Figure S1 and S2) reveals the presence of H-bond networks involving carboxylic oxygen atoms of different substrate anions, which are in agreement with the presence of both monoprotonated [H(2,6-PDC)]$^-$ and completely deprotonated [2,6-PDC]$^{2-}$ forms. Accordingly, the most likely formulation for the crystallized compound is H_5**3**{[H(2,6-PDC)]$_3$(2,6-PDC)}·H_2O·0.5EtOH. This formulation is in agreement with the general behavior observed for [H(2,6-PDC)]$^-$ in the solid state. Indeed, search of the Cambridge Crystallographic Database showed that, with only one exception,[18] in all crystal structures reported for [H(2,6-PDC)]$^-$ this anion adopts a nonzwitterionic form.[19]

Additional H-bond interactions involve carboxylate oxygens with water and EtOH molecules (see the Supporting Information, Table S3).

Proton-Transfer Equilibria of Pyridinedicarboxylate Anions. The protonation constants of pyridinedicarboxylate anions (Supporting Information, Table S4) were determined by means of potentiometric measurements as a preliminary study to investigate the anion binding properties of **1**−**3**. Under the experimental conditions employed, only the first and the second protonation constants of [PDC]$^{2-}$ anions were determined, the third one taking place in very acidic solution. Spectrophotometric (UV) and ^{1}H and ^{13}C NMR measurements performed on these anions at different pH values furnished their protonation patterns (an example is reported in the Supporting Information, Figure S3) showing that first protonation of all PDC anions occurs on the pyridine nitrogen, while the second one involves a carboxylate group. (The carboxylate groups involved in the second protonation of [2,3-PDC]$^{2-}$, [2,4-PDC]$^{2-}$, and [2,5-PDC]$^{2-}$ are those in the positions 3, 2, and 5, respectively, of the pyridine rings, while both groups are similarly implicated in the case of [3,4-PDC]$^{2-}$. For [2,6-PDC]$^{2-}$ and [3,5-PDC]$^{2-}$ the two carboxylate groups are impossible to differentiate due to molecular symmetry.)

It is known that H_2(2,6-PDC) and relevant anions give rise to self-association in aqueous solution. In a previous work,[20] the self-association process was detected by the deviation from the Beer−Lambert law of the variation of molar absorptivity with concentration of H_2(2,6-PDC) in the UV region. The hypochromic and hyperchromic effects, observed at different pH values, were interpreted in terms of different binding interactions, stacking or hydrogen-bonding, occurring in the formation of dimers from different protolytic species. Very high equilibrium constants (log K in the range 6−7) for the formation of such dimers were calculated by using these spectral data.[20]

(18) Aghabozorg, H.; Saei, A. A.; Ramezanipour, F. *Acta Crystallogr. Sect. E: Struct. Rep. Online* **2005**, *61*, o3242.

(19) (a) Moghimi, A.; Sharif, M. A.; Aghabozorg, H. *Acta Crystallogr. Sect. E: Struct. Rep. Online* **2004**, *60*, o1790. (b) Braga, D.; Bazzi, C.; Maini, L.; Grepioni, F. *CrystEngComm* **1999**, *1*, 15. (c) Aghabozorg, H.; Soleimannejad, J.; Sharif, M.; Sheshmani, S.; Moghimi, A. *Anal. Sci.: X-Ray Struct. Anal. Online* **2005**, *21*, x73. (d) Ma, C.-L.; Zhang, J.-H. *Chin. J. Appl. Chem.* **2003**, *20*, 296. (e) Thanigaimani, K.; T. Muthiah, P.; Lynch, D. E. *Acta Crystallogr. Sect. C: Cryst. Struct. Commun.* **2007**, *63*, o295. (f) Moghimi, A.; Sheshmani, S.; Shokrollahi, A.; Shamsipur, M.; Kickelbick, G.; Aghabozorg, H. *Z. Anorg. Allg. Chem.* **2005**, *631*, 160. (g) Aakeroy, C. B.; Hughes, D. P.; McCabe, J. M.; Nieuwenhuyzen, M. *Supramol. Chem.* **1998**, *9*, 127. (h) Aakeroy, C. B.; Hughes, D. P.; McCabe, J. M.; Nieuwenhuyzen, M. *Supramol. Chem.* **1998**, *9*, 127. (i) Aghabozorg, H.; Ghadermazi, M.; Sadr-Khanlou, E. *Anal. Sci.: X-Ray Struct. Anal. Online* **2006**, *22*, x253. (j) Moghimi, A.; Lippolis, V.; Aghabozorg, H.; Shokrollahi, A.; Shamsipur, M.; Sheshmani, S.; Blake, A. J. *Pol. J. Chem.* **2006**, *80*, 1385. (k) Aghabozorg, H.; Ghadermazi, M.; Sheshmani, S. *Anal. Sci.: X-Ray Struct. Anal. Online* **2006**, *22*, x231. (l) Fu, A.-Y.; Wang, D.-Q.; Zhang, C.-L. *Acta Crystallogr. Sect. E: Struct. Rep. Online* **2005**, *61*, o3119. (m) Sheshmani, S.; Ghadermazi, M.; Aghabozorg, H. *Acta Crystallogr. Sect. E: Struct. Rep. Online* **2006**, *62*, o3620. (n) Ng, S. W.; Turnbull, M. M. *Acta Crystallogr. Sect. C: Cryst. Struct. Commun.* **1998**, *54*, 1025.

(20) Peral, F.; Gallego, E. *Spectrochim. Acta Part A* **2000**, *56*, 2149–2155.

TABLE 1. Logarithms of the Equilibrium Constants for the Formation of $[PDC]^{2-}$ (S^{2-}) and $[H(PDC)]^{-}$ (HS^{-}) Complexes with 1−3, Determined in 0.1 M NMe_4NO_3 at 298.1 ± 0.1 K

equilibria	H_2(2,3-PDC)	H_2(2,4-PDC)	H_2(2,5-PDC)	H_2(2,6-PDC)	H_2(3,4-PDC)	H_2(3,5-PDC)
$[H\mathbf{1}]^{+} + S^{2-} = [H\mathbf{1}S]^{-}$	3.4(1)[a]	3.8(1)	3.89(9)	4.19(9)	3.99(7)	4.0(1)
$[H_2\mathbf{1}]^{2+} + S^{2-} = [H_2\mathbf{1}S]$	3.9(1)	4.2(1)	4.2(1)	4.6(1)	4.35(8)	4.2(2)
$[H_3\mathbf{1}]^{3+} + S^{2-} = [H_3\mathbf{1}S]^{+}$	4.6(1)	4.8(1)	5.0(1)	5.3(1)	5.12(9)	5.0(2)
$[H_4\mathbf{1}]^{4+} + S^{2-} = [H_4\mathbf{1}S]^{2+}$						6.6(2)
$[H_3\mathbf{1}]^{3+} + [HS]^{-} = [H_3\mathbf{1}(HS)]^{2+}$	6.4(2)	6.4(2)	6.4(1)	7.5(1)	6.7(1)	
$[H_4\mathbf{1}]^{4+} + [HS]^{-} = [H_4\mathbf{1}(HS)]^{3+}$	6.2(2)	6.2(2)	6.0(1)	7.0(1)	6.4(1)	6.4(2)
$[H_4\mathbf{1}]^{4+} + [H_2S] = [H_4\mathbf{1}(H_2S)]^{4+}$	6.6(2)	6.8(2)	6.7(1)	6.0(1)	6.5(1)	6.7(2)
$[H\mathbf{2}]^{+} + S^{2-} = [H\mathbf{2}S]^{-}$	3.38(9)	2.7(2)	2.84(9)	3.9(2)	2.6(2)	3.2(1)
$[H_2\mathbf{2}]^{2+} + S^{2-} = [H_2\mathbf{2}S]$	3.56(9)	3.2(1)	3.08(7)	3.9(2)	3.0(1)	3.3(1)
$[H_3\mathbf{2}]^{3+} + S^{2-} = [H_3\mathbf{2}S]^{+}$	4.05(8)	3.6(1)	3.54(6)	4.4(2)	3.5(1)	3.5(1)
$[H_4\mathbf{2}]^{4+} + S^{2-} = [H_4\mathbf{2}S]^{2+}$						4.54(3)
$[H_3\mathbf{2}]^{3+} + [HS]^{-} = [H_3\mathbf{2}(HS)]^{2+}$	5.4(1)	4.9(1)	4.75(5)	6.7(2)	4.16(8)	
$[H_4\mathbf{2}]^{4+} + [HS]^{-} = [H_4\mathbf{2}(HS)]^{3+}$	5.0(1)	4.5(1)	4.25(5)	5.2(2)	3.64(4)	3.86(4)
$[H_5\mathbf{2}]^{5+} + [HS]^{-} = [H_5\mathbf{2}(HS)]^{4+}$	5.1(1)	4.9(1)	4.39(6)			
$[H_4\mathbf{2}]^{4+} + [H_2S] = [H_4\mathbf{2}(H_2S)]^{4+}$				5.0(2)		
$[H_2\mathbf{3}]^{2+} + S^{2-} = [H_2\mathbf{3}S]$	2.92(8)	3.4(1)	3.4(1)	3.0(1)	3.4(1)	3.2(1)
$[H_3\mathbf{3}]^{3+} + S^{2-} = [H_3\mathbf{3}S]^{+}$	2.7(1)	3.2(1)	3.3(1)	2.9(1)	3.1(2)	3.0(1)
$[H_4\mathbf{3}]^{4+} + S^{2-} = [H_4\mathbf{3}S]^{2+}$	3.47(7)	4.1(1)	4.1(1)	3.74(9)	4.10(9)	3.9(1)
$[H_5\mathbf{3}]^{5+} + S^{2-} = [H_5\mathbf{3}S]^{3+}$	5.00(7)	5.7(1)	5.8(1)	5.46(9)	5.8(1)	5.8(2)
$[H_5\mathbf{3}]^{5+} + [HS]^{-} = [H_5\mathbf{3}(HS)]^{4+}$	4.67(7)	5.4(1)	5.6(1)	4.88(9)	5.2(1)	5.3(2)
$[H_6\mathbf{3}]^{6+} + [HS]^{-} = [H_6\mathbf{3}(HS)]^{5+}$	4.43(8)	5.7(1)	5.4(1)	4.3(1)	5.1(1)	5.8(2)

[a] Values in parentheses are standard deviations on the last significant figure.

In order to have consistent equilibrium data, in the present work we determined the self-association constants of these species under our experimental conditions (see the Experimental Section). The values we obtained (Table S4, Supporting Information) are significantly lower than the surprisingly high values previously reported. To get confident results, we used both potentiometric and spectrophotometric methods searching for protonation and dimerization constants altogether or as separated entities; a good agreement between the determined values (Table S4, Supporting Information) was obtained. Dimerization was not observed for the other pyridinedicarboxylic isomers.

Binding of $[PDC]^{2-}$ and $[H(PDC)]^{-}$ Anions by 1−3. The stability constants for the binding equilibria of $[PDC]^{2-}$ and $[H(PDC)]^{-}$ anions by protonated forms of **1**−**3** are listed in Table 1.

In order to assess the protonation state of the interacting partners, the binding processes were followed by means of UV spectrophotometric or ^{1}H NMR measurements. UV spectra are diagnostic for protonation of these substrates on the nitrogen atom. Solutions of the completely deprotonated $[PDC]^{2-}$ anions show UV spectra with a band at about 270 nm, due to a $\pi \rightarrow \pi^*$ electronic transition of the pyridine ring, whose molar absorbance (ϵ) is considerably enhanced upon protonation of the pyridine nitrogen. As shown in Figure 2 for the **3**/H_2(2,6-PDC) system, a similar enhancement of ϵ is observed upon the formation of the hexaprotonated complex species, which means that protonation of pentaprotonated form to give the hexaprotonated one takes place on the anion. Hence, the hexaprotonated complex is formed by the $[H(2,6\text{-PDC})]^{-}$ anion (protonated on the pyridine nitrogen) and the $[H_5\mathbf{3}]^{5+}$ receptor form. The same result was found for the complexes of **3** with all anionic substrates (see Supporting Information, Figure S4), and consequently the relevant stability constants were calculated according to the complexation equilibria reported in Table 1. It is to be noted that such proton localization in the complexes is consistent with protonation occurring on the most basic species involved in the complexation reaction.

In the case of **1** and **2**, UV spectra could not be used for the same purpose, since these receptors absorb in the same region

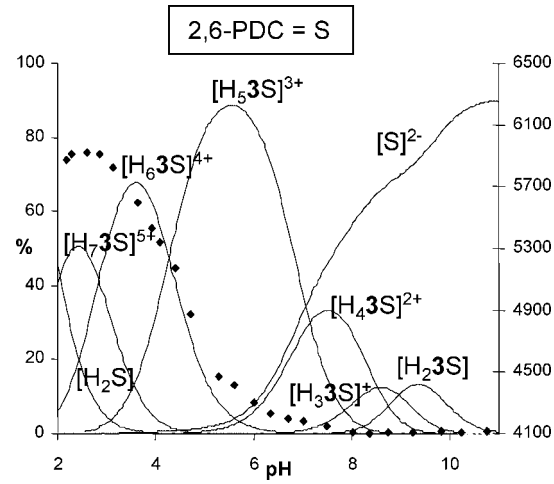

FIGURE 2. Variation with pH of the molar absorptivity (◆ ϵ, $M^{-1}cm^{-1}$) at 272 nm for the systems **3**/H_2(2,6-PDC) superimposed to the distribution diagram of the species present in solution. [**3**] = [H_2(2,6-PDC)] = 1 × 10^{-4} M, 0.1 M NMe_4NO_3, 25 °C.

of the substrates. For this reason, proton localization in the complexes of **1** and **2** was assumed to be regulated by the basicity of the interacting species, as actually occurs for **3**. The complexation equilibria reported in Table 1 for **1** and **2** were written according to this role. In some cases, the protonation pattern of these complexes was confirmed by ^{1}H NMR measurements (Figure 3, Figures S5−S16, Supporting Information), although the interpretation of protonation effects on ^{1}H NMR spectra of the pyridinedicarboxylate anions is complicated by the opposite effect of π-stacking between receptor and substrate aromatic moieties.

π-Stacking interaction between **1**, **2**, and pyridinedicarboxylate substrates is denoted by the upfield shift of ^{1}H NMR signals of all aromatic protons of the interacting partners (Figure 3, Figures S5−S16) indicating that in the complex they are arranged in a face-to-face geometry. The ability of **1** and **2** to give rise to π-stacking interactions characterizes at large extent the binding properties of these receptors. As a matter of fact,

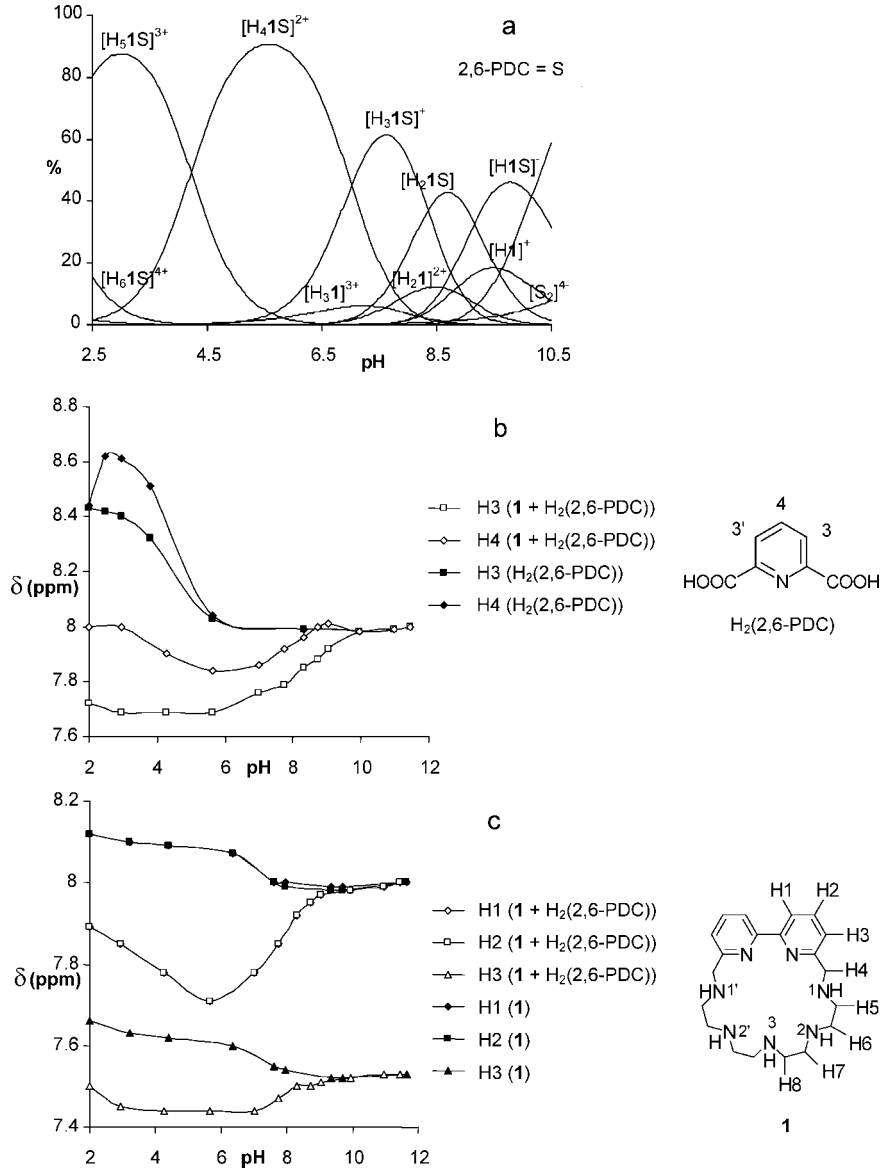

FIGURE 3. System **1**/H_2(2,6-PDC). [**1**] = [H_2(2,6-PDC)] = 1×10^{-3} M, 0.1 M NMe_4NO_3, 25 °C: (a) distribution diagram of the species present in solution as a function of pH; (b) chemical shifts of ^{1}H NMR signals of H_2(2,6-PDC) in the presence and in the absence of **1**; (c) chemical shifts of ^{1}H NMR signals of the aromatic protons of **1** in the presence and in the absence of H_2(2,6-PDC), H1 and H2 signals are coincident.

for equally charged forms of receptors and substrates, **1** and **2** give rise to more stable complexes than **3** (Table 1) which binds the substrates only via charge−charge attraction and hydrogen bonding. For the same reason, **3** needs at least two positive charges to bind the substrates while **1** and **2** are able to form complexes even when they contain a single ammonium group. From an electrostatic point of view, however, a slightly favorable contribution to the stability of **1** and **2** complexes can be expected for some protonated forms of these receptors. Since the heteroaromatic amine groups are less basic than aliphatic ones, the presence of bipyridine and phenanthroline moieties in **1** and **2** forces protonation to occur on the aliphatic chain, thus producing a zone of the receptor with a higher positive charge and more localized charges which interact more strongly with the negative substrates.

The different location of carboxylate/carboxylic groups in substrate structures gives rise to some difference in the stability of the complexes with the same stoichiometry, although the differences are generally not very large and do not follow clear trends. Only in the case of $[2,6\text{-PDC}]^{2-}$ and $[H(2,6\text{-PDC})]^{-}$, the complexes with **1** and **2** are generally more stable than the analogous ones formed by the other substrates, but the same preference is not exhibited by **3**. Since this comparison of complex stability is made under equal, or quite similar, conditions for electrostatic interaction of substrates with the polyammonium receptor chains, the binding preference shown by **1** and **2** for $[2,6\text{-PDC}]^{2-}$ and $[H(2,6\text{-PDC})]^{-}$ species must have its origin in a favorable interaction between the aromatic moieties of the interacting partners, including hydrophobic effects accompanying these association events. As far as the stability constants of the complexes of **1** and **2** with these anions are compared, we observe that **1** exhibits a general greater ability to bind the substrate.

Another interesting feature can be pointed out by comparing the stability constants of complexes with different protonated forms of the substrates. The stability constants of complexes with $[PDC]^{2-}$ dicharged anions increase with the positive charge of the receptors, for all three receptors (Table 1), in agreement

TABLE 2. Logarithms of the Equilibrium Constants for Protonation of Free and Complexed $[PDC]^{2-}$ Anions (S^{2-}), Relevant $\Delta\log K$ and Derived $\Delta G°$ Values (0.1 M NMe_4NO_3, 298.1 ± 0.1 K)

	$[2,3\text{-PDC}]^{2-}$	$[2,4\text{-PDC}]^{2-}$	$[2,5\text{-PDC}]^{2-}$	$[2,6\text{-PDC}]^{2-}$	$[3,4\text{-PDC}]^{2-}$	$[3,5\text{-PDC}]^{2-}$
				log *K*		
$S^{2-} + H^+ = [HS]^-$	4.80(2)[a]	4.81(1)	4.79(2)	4.85(2)	4.94(1)	4.30(2)
$[H_3\mathbf{1}S]^+ + H^+ = [H_3\mathbf{1}(HS)]^{2+}$	6.6(2)	6.4(2)	6.2(1)	7.0(1)	6.5(1)	
$[H_4\mathbf{1}S]^{2+} + H^+ = [H_4\mathbf{1}(HS)]^{3+}$						4.1(1)
$[H_3\mathbf{2}S]^+ + H^+ = [H_3\mathbf{2}(HS)]^{2+}$	6.1(1)	6.1(1)	6.0(1)	7.1(2)	5.6(1)	
$[H_4\mathbf{2}S]^{2+} + H^+ = [H_4\mathbf{2}(HS)]^{3+}$						3.6(1)
$[H_5\mathbf{3}S]^{3+} + H^+ = [H_5\mathbf{3}(HS)]^{4+}$	4.5(1)	4.6(1)	4.6(1)	4.3(1)	4.3(1)	3.8(2)
				$\Delta\log K$		
$\log K_{H_3\mathbf{1}S+H} - \log K_{S+H}$	1.8(2)	1.6(2)	1.4(1)	2.1(1)	1.6(1)	
$\log K_{H_4\mathbf{1}S+H} - \log K_{S+H}$						−0.2(1)
$\log K_{H_3\mathbf{2}S+H} - \log K_{S+H}$	1.3(1)	1.3(1)	1.2(1)	2.2(1)	0.7(1)	
$\log K_{H_4\mathbf{2}S+H} - \log K_{S+H}$						−0.7(2)
$\log K_{H_5\mathbf{3}S+H} - \log K_{S+H}$	−0.3(1)	−0.2(1)	−0.2(1)	−0.6(1)	−0.6(1)	−0.5(2)
				$-\Delta G°$ (kcal/mol)		
$RT(\log K_{H_3\mathbf{1}S+H} - \log K_{S+H})$	2.4(3)	2.2(3)	1.9(1)	2.9(1)	2.2(1)	
$RT(\log K_{H_4\mathbf{1}S+H} - \log K_{S+H})$						−0.3(1)
$RT(\log K_{H_3\mathbf{2}S+H} - \log K_{S+H})$	1.8(1)	1.8(1)	1.6(1)	3.0(1)	0.9(1)	
$RT(\log K_{H_4\mathbf{2}S+H} - \log K_{S+H})$						−0.9(2)
$RT(\log K_{H_5\mathbf{3}S+H} - \log K_{S+H})$	−0.4(1)	−0.3(1)	−0.3(1)	−0.8(1)	−0.8(1)	−0.7(3)

[a] Values in parentheses are standard deviations on the last significant figure

with electrostatic expectations. Nevertheless, when the monoprotonated forms are considered different behaviors are found. In the case of the aliphatic polyamine **3**, the monoprotonated (monocharged) $[H(PDC)]^-$ anions give rise to moderately lower binding constants than the dicharged ones (see equilibria involving $[H_5\mathbf{3}]^{5+}$ in Table 1), as can be expected for an electrostatically driven association process. Conversely, for **1** and **2** containing heteroaromatic groups, the less charged monoprotonated anions (protonated on the pyridine nitrogen) are bound more strongly than the dicharged ones (see equilibria involving $[H_3\mathbf{1}]^{3+}$ and $[H_3\mathbf{2}]^{3+}$ in Table 1) with the unique exception of $[H(3,5\text{-PDC})]^-$ and $[3,5\text{-PDC}]^{2-}$ (see equilibria involving $[H_4\mathbf{1}]^{4+}$ and $[H_4\mathbf{2}]^{4+}$ in Table 1). It is known that pyridinium cations associate more tightly with aromatic groups than uncharged pyridine due to the electron-withdrawing effect of protonation on the π electron density of pyridine and to contributions from cation$-\pi$ interactions which are generally stronger than $\pi-\pi$ interactions.[21,22] Such a difference of interactive forces can be crucial for the association to take place, as recently shown for face-to-face cation$-\pi$ association between pyridinium cations and phenyl groups in crystal structures[21] and edge-to-face in solution.[22] Accordingly, it seems reasonable that the enhanced stability of the complexes with monoprotonated $[HPDC]^-$ anions containing pyridinium groups may have the same origin, although the new arrangement of salt bridges and hydrogen bonds also has to be taken into account.

An estimation of the complex stability enhancement brought about by substrate protonation on the pyridine nitrogen can be obtained by evaluating the free energy change $\Delta G°$ for the metathetic reaction (1), in which the monoprotonated substrate (HS) replaces the completely deprotonated one (S) from the receptor−substrate complex (RS). $\Delta G°$ is given by eq 2, where $\Delta G°_{R+HS}$ and $\Delta G°_{R+S}$ refer to eqs 3 and 4, respectively. Nevertheless, $\Delta G°$ is also given by eq5, where $\Delta G°_{RS+H}$ and $\Delta G°_{S+H}$ refer to eqs 6 and 7, respectively, which accounts for the different basicity of complexed and free substrate. Hence, the difference in basicity between complexed and free substrate, in terms of free energy change, corresponds to the free energy stabilization of the complex brought about by protonation of the coordinated substrate.

$$RS + HS = RHS + S \quad (1)$$

$$\Delta G° = G°_{R+HS} - G°_{R+S} \quad (2)$$

$$R + HS = RHS \quad (3)$$

$$R + S = RS \quad (4)$$

$$\Delta G° = \Delta G°_{RS+H} - \Delta G°_{S+H} \quad (5)$$

$$RS + H = RHS \quad (6)$$

$$S + H = HS \quad (7)$$

The $\Delta G°$ values calculated from eq 5 are reported in Table 2. As can be seen from these data, protonation of the complexed substrate leads to a strengthening of the receptor-substrate interaction by about 1.6−3.0 kcal/mol for the adducts of **1** and **2** with all substrates other than $[3,5\text{-PDC}]^{2-}$, while for $[3,5\text{-PDC}]^{2-}$ and all adducts with **3** it gives rise to a weakening by about 0.3−0.9 kcal/mol. The highest stabilization effect ($\Delta G°$ = 3.0 kcal/mol) is observed for $[2,6\text{-PDC}]^{2-}$ with both **1** and **2**.

To get further information on the binding modes of the interacting partners, we performed a molecular modeling study on the $[H_3\mathbf{1}(2,6\text{-PDC})]^+$, $[H_3\mathbf{1}(H(2,6\text{-PDC}))]^{2+}$, $[H_3\mathbf{2}(2,6\text{-PDC})]^+$, and $[H_3\mathbf{2}(H(2,6\text{-PDC}))]^{2+}$ adducts. Conformational searches carried out on these species evidenced the presence of only one conformational family for each adduct. The lowest energy conformers of the four adducts show similar overall structures (Figure 4) in which the two partners are kept together by hydrogen bonds involving carboxyl groups of the substrate and ammonium/amine groups of the receptor and by rather strong face-to-face π-stacking interactions between their aromatic moieties displaying plane-to-plane distances of about 3.6 Å.

In spite of these similarities, there are significant differences in the calculated structures. In the case of the monoprotonated $[H(2,6\text{-PDC})]^-$ substrate, an additional $NH^+\cdots N$ interaction is

(21) (a) Yamada, S.; Morita, C. *J. Am. Chem. Soc.* **2002**, *124*, 8184–8185. (b) Yamada, S.; Morita, C.; Yamamoto, J. *Tetrahedron Lett.* **2004**, *45*, 7475–7478. (c) Yamada, S.; Morimoto, Y.; Misono, T. *Tetrahedron Lett.* **2005**, *46*, 5673–5676.

(22) Acharya, P.; Plashkevych, O.; Morita, C.; Yamada, S.; Chattopadhyaya, J. *J. Org. Chem.* **2003**, *68*, 1529–1538.

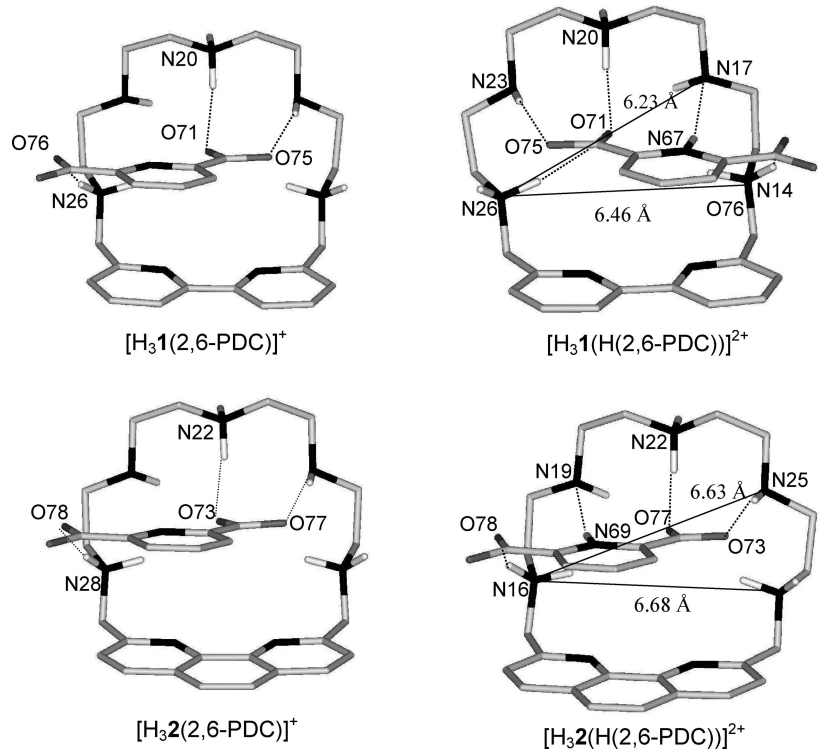

FIGURE 4. Calculated structures of $[H_3\mathbf{1}(2,6\text{-PDC})]^+$, $[H_3\mathbf{1}(H(2,6\text{-PDC}))]^{2+}$, $[H_3\mathbf{2}(2,6\text{-PDC})]^+$, and $[H_3\mathbf{2}(H(2,6\text{-PDC}))]^{2+}$ adducts.

established between the protonated pyridine nitrogen and one unprotonated aliphatic nitrogen of $[H_3\mathbf{1}]^{3+}$ and $[H_3\mathbf{2}]^{3+}$. In $[H_3\mathbf{1}(H(2,6\text{-PDC}))]^{2+}$, the $[H(2,6\text{-PDC})]^-$ substrate bridges the two protonated pseudobenzylic nitrogens of **1** located 6.46 Å apart from each other (Figure 4). On the other hand, in $[H_3\mathbf{2}(H(2,6\text{-PDC}))]^{2+}$, the distance between the two pseudobenzylic nitrogens is longer (6.68 Å), probably because of the greater rigidity of the phenanthroline moiety compared to the bipyridine one, and $[H(2,6\text{-PDC})]^-$ prefers to bridge the N16 ammonium group and the N25 amine nitrogen of $[H_3\mathbf{2}]^{3+}$ (Figure 4). As a consequence, the $[H_3\mathbf{1}(H(2,6\text{-PDC}))]^{2+}$ species gives rise to a higher number of hydrogen bond contacts than $[H_3\mathbf{2}(H(2,6\text{-PDC}))]^{2+}$ and involves three ammonium groups of the receptor instead of two (Figure 4, Table S5 in the Supporting Information) in the formation of $NH^+\cdots O^-$ salt bridges. Moreover, as shown in Figure 5, in $[H_3\mathbf{1}(H(2,6\text{-PDC}))]^{2+}$ and $[H_3\mathbf{2}(H(2,6\text{-PDC}))]^{2+}$, the acidic proton of $[H(2,6\text{-PDC})]^-$ is located above one heteroaromatic nitrogen of the receptors, which is rich in electron density because of its high electronegativity, giving rise to additional favorable electrostatic interactions, as compared to $[H_3\mathbf{1}(2,6\text{-PDC})]^+$ and $[H_3\mathbf{2}(2,6\text{-PDC})]^+$.

The results of this modeling study are in good agreement with the general features, outlined by thermodynamic and spectroscopic methods, of these substrate−receptor complexes assembled through the formation of a number of salt bridges and hydrogen bonds and π-stacking association of the aromatic moieties, and furnish some elements to explain particular aspects of these complex stability. Accordingly, the increased complex stability observed upon substrate protonation can be associated to the higher number of binding contacts formed with the receptor by the protonated substrates, and the greater binding ability of **1** toward 2,6-pyridinedicarboxylate anions, with respect to **2**, can be explained by taking into account the involvement by **1** of a greater number of salt bridges and hydrogen bonds probably resulting from a more appropriate size of **1**.

Binding Selectivity. The stability constant determined for each complex species is the result of the different binding or repulsive forces acting between substrate and receptor and of all effects involving molecular constrains and solvation/desolvation processes accompanying the association event. All these contributions to complex stability are generally dependent on the environmental conditions (pH, concentrations, protonation state, etc.). Hence, a mere comparison of the stability constants of analogous complexes gives us information on their binding ability out of the environmental context, that is, it answers the questions "which binds better?" or "which is bound better?", but it cannot answer the question "which is selectively bound?" since selective binding (recognition) is strongly affected by the environmental context. The compared complexes, although they have strict analogies, may exist under different environmental conditions and be involved in different concomitant equilibria. For this reason, the straightforward comparison of stability constants is generally an improper method to analyze selectivity in complex systems, in particular for complex systems, like those ones studied here, where both substrates and receptors are involved in multiple protonation equilibria. The best way to analyze selectivity in similar systems would be to perform actual competitive experiments, but unfortunately, when the competitive systems are complicated like those studied here, such direct experiments are not amenable to analysis or do not furnish confident results. When actual competitive experiments are not beneficial, a useful computational method[23] balancing all

(23) (a) Bianchi, A.; Garcia-España, E. *J. Chem. Educ.* **1999**, *76*, 1727–1732. (b) Bencini, A.; Bianchi, A.; Burguete, M. I.; Dapporto, P.; Domenech, A.; Garcia-España, E.; Luis, S. V.; Paoli, P.; Ramirez, J. A. *J. Chem. Soc., Perkin Trans. 2* **1994**, 569–577.

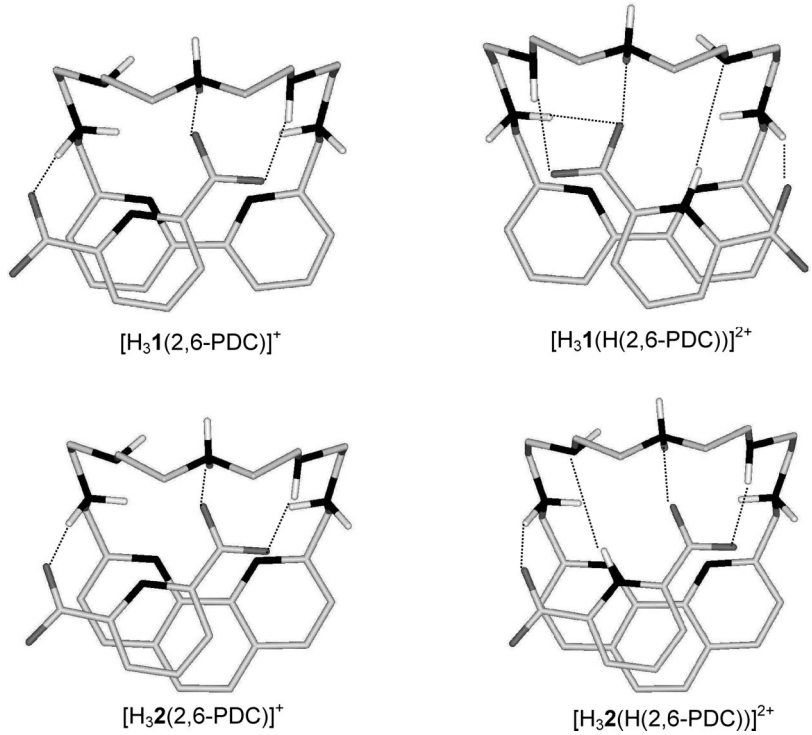

FIGURE 5. Top view of the calculated structures of $[H_3\mathbf{1}(2,6\text{-PDC})]^+$, $[H_3\mathbf{1}(H(2,6\text{-PDC}))]^{2+}$, $[H_3\mathbf{2}(2,6\text{-PDC})]^+$, and $[H_3\mathbf{2}(H(2,6\text{-PDC}))]^{2+}$ adducts.

complex stability constants along with receptors and substrates basicity can be used to calculate the percentage of the species formed, as a function of pH, in competitive systems containing receptors and substrates being compared and plot the overall percentages of the complexes formed by the competing reactants vs pH. This criterion allows for attributing selectivity over all the pH range. When the formation of species different from those found in the noncompetitive systems is reasonably improbable, like in the present cases, this method furnishes confident results.

Examples of similar competitive diagrams obtained for each of the three receptors in the presence of equimolar amounts of the six substrates are reported in Figure 6. As can be seen, **3** does not show binding selectivity toward any particular substrate, although it displays some preference for anions deriving from H_2(2,4-PDC), H_2(2,5-PDC), H_2(3,4-PDC), and H_2(3,5-PDC), while **1** and **2** recognize the anionic forms of H_2(2,6-PDC) over a large pH range.

As far as the selectivity of the three receptors in the binding of 2,6-pyridinedicarboxylate anions is concerned, a selectivity diagram (Figure 7) calculated for a solution containing H_2(2,6-PDC), **1**, **2**, and **3** in equimolar concentrations clearly points out the higher efficiency of **1** in recognizing the substrate increasingly from alkaline to acidic solutions where **1** strongly competes with the other receptors as much as to bind about 90% of the substrate. Such behavior is in agreement with the higher stability of **1** complexes which increases more rapidly on lowering the solution pH, when complexes containing the receptors in their high protonation states are formed.

Conclusions

The three polyammonium receptors studied in this work are efficient receptors for pyridinedicarboxylate substrates even in a solvent like water, which reduces at large extent the electrostatic attraction between the interacting partners and strongly competes with their association via hydrogen bonding. Nevertheless, the formation of complex adducts characterized by considerable stability is made possible by the high number of salt bridges and hydrogen bond contacts taking place between the cationic receptors and the anionic substrates, as shown in the solid state by the crystal structure of $H_8[\mathbf{3}(2,6\text{-PDC})_4]\cdot H_2O\cdot 0.5EtOH$.

Among pyridinedicarboxylate isomers, $[2,6\text{-PDC}]^{2-}$ and $[H(2,6\text{-PDC})]^-$ are efficiently recognized by **1** and **2**. As shown by the crystal structure, these substrates show a highly preorganized structure for interaction with similar receptors, the two carboxylate groups and the pyridine nitrogen being conveniently arranged for a synergetic binding action. The resulting binding mode promoted by these groups orientates the aromatic ring in such a way that strong π-stacking association with the aromatic moieties of **1** and **2** can occur, affording an additional contribution to complex stability which is favored by the polar character of water. Moreover, the pyridine nitrogen of the substrate is appropriately positioned to further stabilize the adduct, upon protonation (formation of a pyridinium group), through the formation of additional $NH^+\cdots N$ hydrogen bonds with the receptor and electrostatic attraction between the pyridinium group and the electron-rich aromatic nitrogens of **1** and **2**.

Compound **1** binds 2,6-pyridinedicarboxylate anions more efficiently than **2** over a large pH range, being the best receptor among those studied here. A better size matching between substrate and receptor promoted by the lower rigidity of the bipyridine moiety of **1**, compared to phenanthroline in **2**, allowing the formation of more and stronger binding contacts, seems to be at the origin of the enhanced selectivity of **1**.

According to these results, the present receptors containing heteroaromatic groups, in particular **1**, are promising candidates

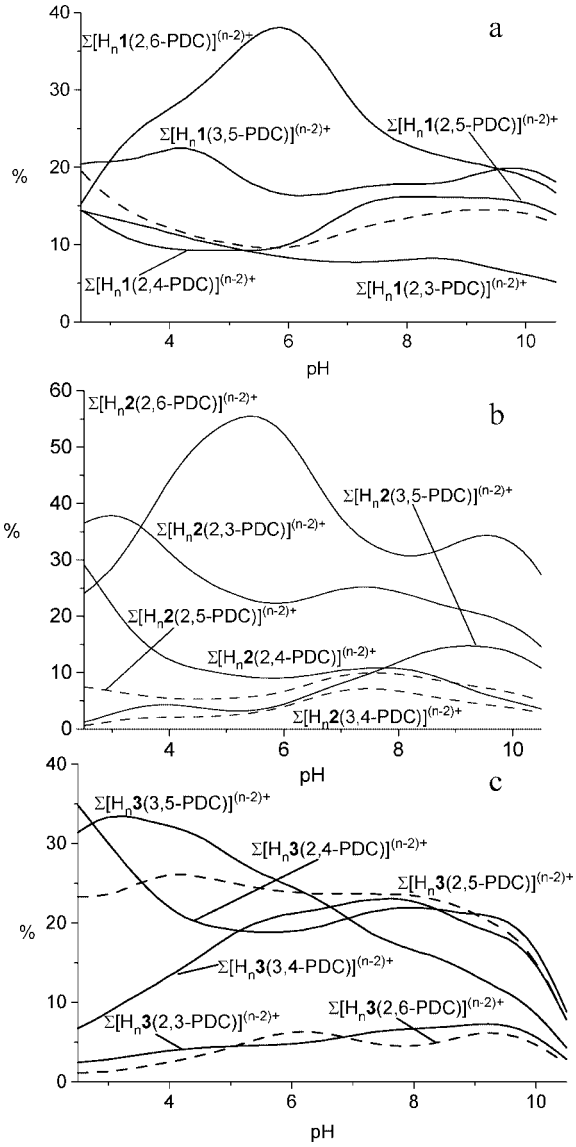

FIGURE 6. Selectivity diagrams calculated for the systems (a) **1**/H_2PDC and (b) **2**/H_2PDC, **3**/H_2PDC showing the percentage of the overall concentration of receptor (**1**−**3**) bound to each substrates, in the presence of all substrates, as a function of pH. All reagents 1×10^{-3} M.

to develop new functionalized receptors bearing sensing units for rapid detection of H_2(2,6-PDC). We are currently studying this aspect.

Experimental Section

General Methods. Receptors **1**,[24] **2**,[25] and **3**,[26] employed to perform the potentiometric measurements, were synthesized according to described procedures and used as (H_5**1**)Br_5, (H_5**2**)Br_5, and (H_7**3**)Cl_7. High purity (≥99%) pyridinedicarboxylic acids were purchased from a commercial supplier.

Crystals of H_8[**3**(2,6-PDC)$_4$]·H_2O·0.5EtOH suitable for X-ray analysis were obtained by slow evaporation at room temperature of a ethanol/water solution containing **3** and 4 equiv of H_2(2,6-PDC).

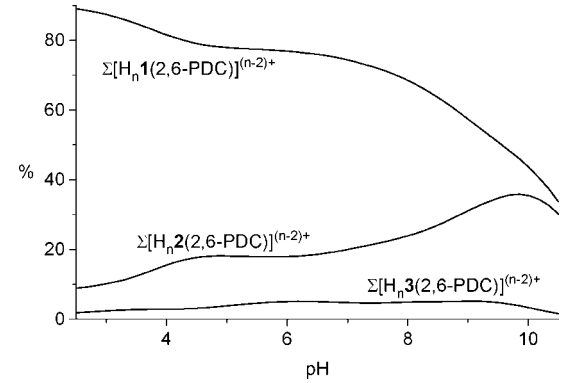

FIGURE 7. Selectivity diagram calculated for the system **1**/**2**/**3**/H_2(2,6-PDC) showing the percentage of the overall concentration of substrate bound to each receptor, in the presence of all receptors, as a function of pH. All reagents 1×10^{-3} M.

X-ray Structure Analyses. A single crystal of H_8[**3**(2,6-PDC)$_4$]·H_2O·0.5EtOH was analyzed by means of X-ray crystallography at low temperature (T = 150 K). A summary of the crystallographic data is reported in the Supporting Information (Table S6). The intensities of some reflections were monitored during data collection to check the stability of the crystal: no loss of intensity was observed. The integrated intensities were corrected for Lorentz and polarization effects and empirical absorption correction was applied by means of ABSPACK program.[27] The structure were solved by direct methods (SIR97).[28] Refinement was performed by means of full-matrix least-squares using SHELX-97 program.[29] All the non-hydrogen atoms were anisotropically refined while the hydrogen atoms linked to carbon atoms, nitrogen atoms, and alcoholic oxygen were introduced in calculated positions and their coordinates were refined according to the linked atoms. Positions of the acidic protons of the macrocyclic receptors have been deduced from interactions found during crystal packing analysis. The acidic protons of the monoprotonated [H(2,6-PDC)]$^-$ anions were not localized in the ΔF map carried out at the end of refinement, and accordingly, they were not introduced in calculations. Due to the high number of low intensity reflections at high values of ϑ, reflections with sin ϑ/λ higher than 0.5 (d = 1 Å) were not used during refinement. Unfortunately the low quality of data led to rather high values for the agreement factors and high esd values for bond lengths.

Potentiometric Measurements. All pH-metric measurements (pH = −log [H^+]) employed for the determination of equilibrium constants were carried out in 0.1 M NMe_4NO_3 solutions at 298.1 ± 0.1 K by using the equipment and the methodology that has been already described.[30] The combined glass electrode was calibrated as a hydrogen concentration probe by titrating known amounts of HCl with CO_2-free NMe_4OH solutions and determining the equivalent point by Gran's method[31] which allows one to determine the standard potential $E°$ and the ionic product of water (pK_w = 13.83(1) at 298.10.1 K in 0.1 M NMe_4NO_3). At least three measurements were performed for each system in the pH ranges 2.5−10.5. In all experiments the receptor concentration [R] was about 1×10^{-3} M while the concentration of PDC acids was varied in the range [R] ≤ [PDC] ≤ 3[R]. Experiments for the determination of PDC acidity constants were performed by using 1×10^{-3} M

(24) Bencini, A.; Bianchi, A.; Giorgi, C.; Fusi, V.; Masotti, A.; Paoletti, P. *J. Org. Chem.* **2000**, *65*, 7686–7689.
(25) Bazzicalupi, C.; Bencini, A.; Fusi, V.; Giorgi, C.; Paoletti, P.; Valtancoli, B. *Inorg. Chem.* **1998**, *37*, 941–948.
(26) Micheloni, M.; Paoletti, P.; Bianchi, A. *Inorg. Chem.* **1985**, *24*, 3702–3704.
(27) Multiscan Procedure; CrysAlis Pro v 1.171.29.2 Oxford Diffraction LTD, Abington, OxfordShire, England, 2006.
(28) Altomare, A.; Burla, M. C.; Camalli, M.; Cascarano, G. L.; Giacovazzo, C.; Gagliardi, A.; Moliterni, A. G. G.; Polidori, G.; Spagna, R. *J. Appl. Crystallogr.* **1999**, *32*, 115.
(29) Sheldrick, G. M. SHELXL-97; Göttingen, Germany, 1997.
(30) Bianchi, A.; Bologni, L.; Dapporto, P.; Micheloni, M.; Paoletti, P. *Inorg. Chem.* **1984**, *23*, 1201–1205.
(31) (a) Gran, G. *Analyst (London)* **1952**, *77*, 661–671. (b) Rossotti, F. J.; Rossotti, H. *J. Chem. Educ.* **1965**, *42*, 375–378.

solutions of these compounds. Only in the case of H_2(2,6-PDC), which gives rise to self-aggregation equilibria, its concentration was varied in the range $0.01-1 \times 10^{-4}$ M to follow the dimerization process. The stability constants were calculated from the emf data by means of the computer program HYPERQUAD,[32] a general program for equilibrium constants computation. The core of the algorithm is a Gauss−Newton nonlinear least-squares minimization of a sum of weighted squared residuals in electrode potentials. The refinement is protected against divergence according to the procedure outlined by Marquardt.[33] All the required derivatives are obtained analytically. The unknown free reactant concentrations are calculated by simultaneous solution of the nonlinear mass-balance equations using the Newton−Raphson procedure.

Examples of titration data and fitting results for the complex systems are reported in the Supporting Information (Figures S17−S19). Protonation constants and complex stability constants were determined with separate experiments. In the case of complexation data, only the stability constants of the complex species were refined, while protonation constants of substrates and receptors were kept constant. In such a way, at most four complexation constants were determined simultaneously. On the basis of a critical evaluation of the least-squares results and of the statistical analysis of the weighted residuals supplied by the HYPERQUAD[32] program, we considered acceptable only those models for which the value of the variance of the residuals σ^2 was not greater that 9 (estimated errors of 0.3 mV on the emf readings and 0.003 cm^3 on the titrant volume). Different equilibrium models for complex formation were produced, to account for different protonation states of the complexes and different receptor-to-substrate stoichiometries. When more than one model gave a σ^2 value within the accepted level, the model selection was made by performing an F test.[34] To further control the consistency of the experimental data, the protonation and complex formation curves, for each system, were collected together in a unique set of data and all the equilibrium constants simultaneously refined. The equilibrium constants obtained were equal, within the standard deviations, to those obtained by treating protonation data and complex formation data as separated sets of data.

Spectrophotometric Measurements. All spectrophotometric measurements were performed in 0.1 M NMe_4NO_3 solutions at 298.1 ± 0.1 K. Spectrophotometric titrations used to determine the acidity and dimerization constants of 2,6-PDC (see the Supporting Information, Figure S20) were performed at fixed pH values (pH 1, 3.9, 9.0) and with a concentration of 2,6-PDC in the range $1.6 \times 10^{-5}-3.8 \times 10^{-4}$ M (pH 1), $1.6 \times 10^{-5}-3.0 \times 10^{-4}$ M (pH 3.9), or $1.6 \times 10^{-5}-4.3 \times 10^{-4}$ M (pH 9.0). Spectra of samples with different H_2(2,6-PDC) concentrations were recorded for each pH value in the range 250−300 nm analyzed with SpecFit32 program,[35] by which the absorptivities and the stability constants of the species formed at equilibrium were adjusted. This program uses factor analysis to reduce the absorbance matrix and to extract the eigenvalue prior to fit of the reduced data set according to the Marquardt algorithm.[34] An example of fitting performed with data obtained at 271 nm is reported in Figure S20 (Supporting Information). Model selection was performed by using the same criterion adopted for potentiometric measurements.

^{1}H and ^{13}C NMR Measurements. ^{1}H and ^{13}C NMR spectra were recorded at 298 K on a 300 MHz instrument. In the ^{1}H NMR spectra, peak positions are reported relative to HOD at δ 4.79 ppm (D_2O), while in ^{13}C spectra peak positions are reported relative to 1,4-dioxane at δ 67.2 ppm (D_2O). In the pH-metric titrations, small amounts of 0.01 M NMe_4OD or DCl were added to adjust the pD. The pH was calculated from the measured pD value by using the relationship pH = pD − 0.40.[36]

Molecular Modeling. Conformational searches were carried out, by means of the simulated annealing method, on the $[H_3\mathbf{1}$(2,6-PDC)$]^+$, $[H_3\mathbf{1}$(H(2,6-PDC))$]^{2+}$, $[H_3\mathbf{2}$(2,6-PDC)$]^+$, and $[H_3\mathbf{2}$(H(2,6-PDC))$]^{2+}$ adducts. CHARMM27[37] force field, as implemented in Hyperchem 7.51,[38] was employed with $\varepsilon = 4R$ and atomic charges calculated by PM3[39] semiempirical method. Energy minimizations were performed using a conjugate gradient algorithm (0.001 kcal/Å mol). Each search was carried out by using starting and final T = 0 K, running T = 600 K, heating, cooling and running time = 10 ps, time step = 1 fs. From each conformational search, 80 conformers were obtained and collected in families with rms threshold value of 0.8 for all non-hydrogen atoms. Cartesian coordinates for the calculated structures are reported in the Supporting Information (Tables S7−S10).

Acknowledgment. Financial support from CTQ2006-15672-CO5-01 (Spain) is gratefully acknowledged.

Supporting Information Available: Selected H-bond distances (Table S1) and torsional angles (Table S2) for $H_8[\mathbf{3}$(2,6-PDC)$_4]\cdot H_2O\cdot$0.5EtOH, H-bond interactions in the crystal packing of $H_8[\mathbf{3}$(2,6-PDC)$_4]\cdot H_2O\cdot$0.5EtOH (Table S3), equilibrium constants for protonation of $[PDC]^{2-}$ and $[HPDC]^-$ anions and 2,6-PDC self-association (Table S4), selected H-bond distances for the calculated structures of $[H_3\mathbf{1}$(2,6-PDC)$]^+$, $[H_3\mathbf{1}$(H(2,6-PDC))$]^{2+}$, $[H_3\mathbf{2}$(2,6-PDC)$]^+$, and $[H_3\mathbf{2}$(H(2,6-PDC))$]^{2+}$ (Table S5), crystallographic data for $H_8[\mathbf{3}$(2,6-PDC)$_4]\cdot H_2O\cdot$0.5EtOH (Table S6), Cartesian coordinates for the calculated structures of $[H_3\mathbf{1}$(2,6-PDC)$]^+$, $[H_3\mathbf{1}$(H(2,6-PDC))$]^{2+}$, $[H_3\mathbf{2}$(2,6-PDC)$]^+$, and $[H_3\mathbf{2}$(H(2,6-PDC))$]^{2+}$ (Tables S7−S10), part of the crystal packing of $H_8[\mathbf{3}$(2,6-PDC)$_4]\cdot H_2O\cdot$0.5EtOH and O···H···O (Figures S1 and S2), UV, ^{1}H and ^{13}C NMR data for the protonation of $[2,3\text{-PDC}]^{2-}$ (Figure S3), variation with pH of the molar absorptivity of the systems **3**/H_2PDC (Figure S4), distribution diagrams and ^{1}H NMR data at various pHs for all complex systems with **1** (Figures S5−S10) and **2** (Figures S11−S16), potentiometric titration data for the determination of complex stability constants (Figure S20−S22), and UV−vis titration data for the determination of self-association constants of H_2(2,6-PDC) in aqueous solution (Figure S23). This material is available free of charge via the Internet at http://pubs.acs.org.

JO801366W

(32) Gans, P.; Sabatini, A.; Vacca, A. *Talanta* **1996**, *43*, 1739–1753.
(33) Marquardt, D. W. *J. Soc. Ind. Appl. Math.* **1963**, *11*, 431–441.
(34) Freund, J. E. *Mathematical Statistics*; Prentice Hall: New York, 1962.
(35) SPECFIT/32, Global Analysis System, v.3.0, Spectrum Associates, Marlborough, MA, USA, http://www.bio-logic.info/rapid-kinetics/software.html.
(36) Covington, A. K.; Paabo, M.; Robinson, R. A.; Bates, R. G. *Anal. Chem.* **1968**, *40*, 700–706.
(37) (a) Brooks, B. R.; Bruccoleri, R. E.; Olafson, B. D.; States, D. J.; Swaminathan, S.; Karplus, M. *J. Comput. Chem.* **1983**, *4*, 187–217. (b) Smith, J. C.; Karplus, M. *J. Am. Chem. Soc.* **1992**, *114*, 805–812.
(38) Hyperchem β1 Release 7.51 (2002) for Windows Molecular Modelling System, Hypercube, Inc., Gainsville, FL, 32601.
(39) Stewart, J. P. P. *J. Comput.-Aided Mol. Des.* **1990**, *4*, 1–105.